Electronic Supplementary Material (ESI) for Physical Chemistry Chemical Physics.

Supporting Information for "II. Dissociation free energies in drug-receptor systems via non equilibrium alchemical simulations: application to the FK506-related immunophilin ligands."

Francesca Nerattini,[†,‡] Riccardo Chelli,[†] and Piero Procacci[*,†]

Department of Chemistry, University of Florence, Italy, and Department of Physics, University of Vienna, Boltzmanngasse 5 1090 Vienna, Austria

E-mail: procacci@unifi.it

Dissociation free energy in systems with two competing binding poses

Assuming for the sake of simplicity and with no loss of generality that only two binding poses exist, then the annihilation work distribution would be correspondingly made of two normal components due to the bound state and one shadow state (for standard MD boxes) due to the unbound pair

$$P(W_{1\to 0}) = c_{b1}N_{b1}(W) + c_{b2}N_{b2}(W) + c_sN_s(W) \tag{1}$$

*To whom correspondence should be addressed
†Dept. of Chemistry, University of Florence, Italy
‡Dept. of Physics, University of Vienna, Austria

We further assume, again with no loss of generality, that the two normal components referring to the bound state have different mean values, $\langle W_{1\to 0}^{(b1)}\rangle$, $\langle W_{1\to 0}^{(b2)}\rangle$, and equal σ's, yielding a volume dependent dissociation free energy given by

$$\Delta G_{\rm box} \;=\; -k_B T \ln\left[c_{b1} e^{-\beta\Delta G_{b1}}\left(1+\frac{c_{b2}}{c_{b1}}e^{-\beta(\Delta G_{b2}-\Delta G_{b1})}+\frac{c_s}{c_{b1}}e^{-\beta(\Delta G_s-\Delta G_{b1})}\right)\right] \tag{2}$$

where $\Delta G_{b1/2} = \langle W_{1\to 0}^{(b1/2)}\rangle - \frac{1}{2}\beta\sigma^2$ are the dissociation free energies of the two poses. The probability ratio between the two mutually exclusive poses is given by $c_{b2}/c_{b1} = e^{-\beta(\Delta G_{b1}-\Delta G_{b2})}$. Here we are implicitly assuming that the annihilation process is so fast that no mixing occurs between the two poses. This can be easily verified as the cumulants of the two components mixture must satisfy the relation

$$\frac{c_{b2}}{c_{b1}} = e^{\beta(\Delta G_{b2}-\Delta G_{b1})} = e^{\beta(\langle W_{1\to 0}^{(b2)}\rangle - \langle W_{1\to 0}^{(b1)}\rangle)} \tag{3}$$

According to the no mixing hypothesis we have that $\frac{c_b}{c_s} = e^{\beta[(\Delta G_b-\Delta G_s)-k_B T\ln V_{\rm box}/V_{\rm site}]}$. It then follows that the ratio between the *cumulative* bound states and unbound states is given by

$$\frac{c_{b1}+c_{b2}}{c_s} = e^{\beta[(\Delta G_b-\Delta G_s)-k_B T\ln V_{\rm box}/V_{\rm site}]} \tag{4}$$

Exploiting in the above equation the relation[1] $e^{\beta\Delta G_b} = e^{\beta\Delta G_{b1}} + e^{\beta\Delta G_{b2}}$, we obtain

$$\frac{c_{b1}}{c_s}+\frac{c_{b2}}{c_s} = e^{\beta[(\Delta G_{b1}-\Delta G_s)-k_B T\ln V_{\rm box}/V_{\rm site}]} + e^{\beta[(\Delta G_{b2}-\Delta G_s)-k_B T\ln V_{\rm box}/V_{\rm site}]} \tag{5}$$

so that

$$\frac{c_{b1/2}}{c_s} = e^{\beta[(\Delta G_{b1/2}-\Delta G_s)-k_B T\ln V_{\rm box}/V_{\rm site}]} \tag{6}$$

Using Eqs. 6 and 3 in Eq. 2 and using the fact $c_{b1}+c_{b2}+c_s = 1$, we finally find

$$\Delta G_{\rm box} = \Delta G_s + k_B T \ln\left(\frac{e^{\beta(\Delta G_{b1}-\Delta G_s)}+e^{\beta(\Delta G_{b2}-\Delta G_s)}+\frac{V_{\rm box}}{V_{\rm site}}}{2+\frac{V_{\rm box}}{V_{\rm site}}}\right) \tag{7}$$

If $V_{\rm box} \gg V_{\rm site}$ and if the tight binding ligand hypothesis holds ($e^{\beta(\Delta G_{b1}-\Delta G_s)} \gg V_{\rm box}/V_{\rm site}$) with the secondary binding pose being such that $e^{-\beta(\Delta G_{b1}-\Delta G_{b2})} \ll 1$, we obtain

$$\Delta G_{\rm box} = \Delta G_{b1} - k_B T \ln \frac{V_{\rm box}}{V_{\rm site}} \tag{8}$$

with the dissociation free energy being dominated by the largest component ΔG_{b1}. If the two poses have comparable probability ratio, then the (volume independent) annihilation free energy of the complex is given by

$$\Delta G_b \;=\; -k_B T \ln \frac{1}{e^{\beta \Delta G_{b1}} + e^{\beta \Delta G_{b2}}} \tag{9}$$

Exploiting the tight binding ligand hypothesis, i.e. $c_{b1} + c_{b2} \simeq 1$ and assuming the no mixing hypothesis with $c_{b1/2} = \frac{e^{\beta \Delta G_{b1/2}}}{e^{\beta \Delta G_{b1}} + e^{\beta \Delta G_{b2}}}$, Eq. 9 can be rearranged as

$$\Delta G_b \;=\; -k_B T \ln(c_{b1} e^{-\beta \Delta G_{b1}} + c_{b2} e^{-\beta \Delta G_{b2}}) - k_B T \ln 2 \tag{10}$$

Note that the first term in Eq. 10 is the Crooks-based free energy for the two component mixture, $c_{b1} N_{b1}(W) + c_{b2} N_{b2}(W)$, as if the third shadow component in Eq. 1, $N_s(W)$, due to the unbound states were not present. The shadow component gets exponentially amplified in the reverse process, hence diminishing the weight of the bound state normal components in $P(-W_{0\to 1})$ and red-shifting the overall dissociation free energy by the quantity $-k_B T \ln 2 = -0.41$ kcal mol^{-1}.

Force field parameters for the FK506 ligand

Fig. S1 shows FK506 structure and atom name assignment. The topology file containing atom type assignment, atomic charges (in electrons), bonds and improper dihedrals is reported below in the ORAC topology ready-to-use file format.[2]

```
RESIDUE fk5 ( Total charge = 0.0 )
atoms
```

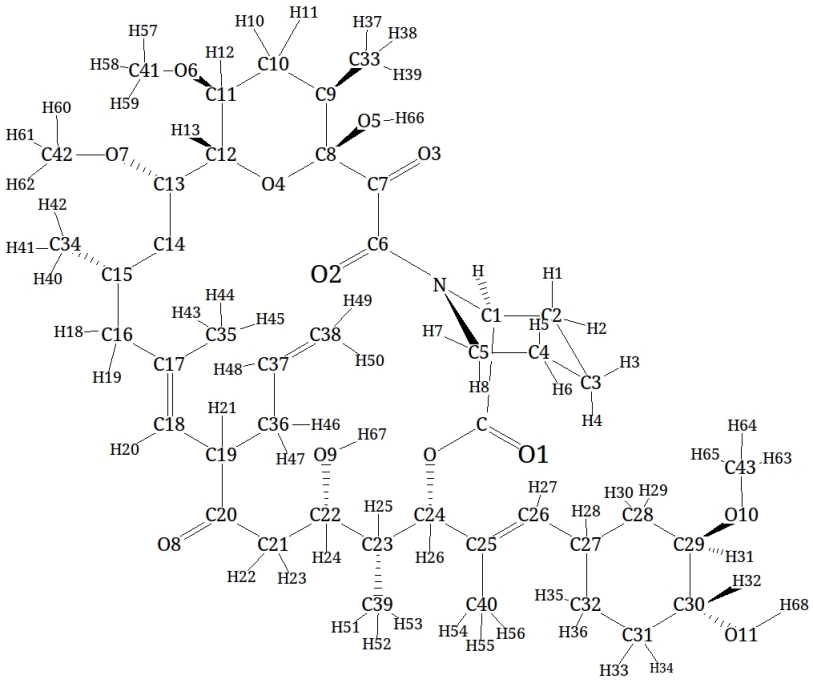

Figure S1: FK506 structure and atom name assignment.

```
group
c43 ct 0.009839
h63 h1 0.054354
h64 h1 0.054354
h65 h1 0.054354
group
o10 os -0.402630
group
c29 ct 0.151941
h31 h1 0.059222
group
c28 ct -0.328596
h29 hc 0.111764
h30 hc 0.111764
group
c30 ct 0.267598
h32 h1 0.073931
group
o11 oh -0.683716
h68 ho 0.421585
group
c31 ct -0.186554
h33 hc 0.055232
```

```
h34 hc 0.055232
group
c32 ct -0.112822
h35 hc 0.036500
h36 hc 0.036500
group
c27 ct 0.451132
h28 hc -0.039679
group
c26 cd -0.424141
h27 ha 0.136133
group
c25 cd -0.310860
group
c40 ct 0.309277
h54 hc -0.083945
h55 hc -0.083945
h56 hc -0.083945
group
c24 ct 0.707507
h26 h1 -0.016347
group
c23 ct -0.461096
h25 hc 0.086512
group
c39 ct -0.576486
h51 hc 0.178268
h52 hc 0.178268
h53 hc 0.178268
group
c22 ct 0.613751
h24 h1 0.033569
group
o9 oh -0.745315
h67 ho 0.460501
group
c21 ct -0.503356
h22 hc 0.132798
h23 hc 0.146218
group
c20 c 0.459991
o8 o -0.451160
group
```

```
c19 ct 0.095111
h21 hc 0.043008
group
c36 ct 0.054119
h46 hc 0.017944
h47 hc 0.058513
group
c37 cd -0.186805
h48 ha 0.147818
group
c38 cd -0.403838
h49 ha 0.164669
h50 ha 0.161278
group
c18 cd -0.449082
h20 ha 0.056397
group
c17 cd 0.383379
group
c35 ct -0.470982
h43 hc 0.124842
h44 hc 0.124842
h45 hc 0.124842
group
c16 ct -0.486783
h18 hc 0.086000
h19 hc 0.102940
group
c15 ct 0.619762
h17 hc -0.110942
group
c34 ct -0.495335
h40 hc 0.103960
h41 hc 0.103960
h42 hc 0.103960
group
c14 ct -0.153620
h15 hc 0.335182
h16 hc -0.069880
group
c13 ct -0.050163
h14 h1 0.075434
group
```

```
o7 os -0.172190
group
c42 ct -0.179544
h60 h1 0.086298
h61 h1 0.086298
h62 h1 0.086298
group
c12 ct 0.212721
h13 h1 0.090470
group
c11 ct 0.089178
h12 h1 0.078879
group
o6 os -0.337219
group
c41 ct -0.039709
h57 h1 0.061005
h58 h1 0.061005
h59 h1 0.061005
group
c10 ct -0.396967
h10 hc 0.134183
h11 hc 0.134183
group
c9 ct 0.375589
h9 hc -0.001053
group
c33 ct -0.460209
h37 hc 0.106486
h38 hc 0.106486
h39 hc 0.106486
group
c8 ct 0.248853
group
o5 oh -0.615804
h66 ho 0.432026
group
o4 os -0.436293
group
c7 c 0.454736
o3 o -0.445279
group
c6 c 0.342605
```

```
o2 o -0.491689
group
n n -0.096506
group
c1 ct -0.015294
h h1 0.104747
group
c2 ct -0.107551
h1 hc 0.058353
h2 hc 0.058353
group
c3 ct 0.106273
h3 hc 0.001525
h4 hc 0.001525
group
c4 ct -0.191232
h5 hc 0.075250
h6 hc 0.075250
group
c5 ct -0.091625
h7 h1 0.080421
h8 h1 0.080421
group
c c 0.486970
o1 o -0.514691
group
o os -0.233834
end

bonds
c c1 c o c o1
c1 c2 c1 n c1 h
c2 c3 c2 h1 c2 h2
c3 c4 c3 h3 c3 h4
c4 c5 c4 h5 c4 h6
c5 n c5 h7 c5 h8
c6 c7 c6 n c6 o2
c7 c8 c7 o3
c8 c9 c8 o4 c8 o5
o5 h66
c9 c10 c9 c33 c9 h9
c33 h39 c33 h38 c33 h37
c10 h11 c10 h10 c10 c11
```

```
c11 h12 c11 o6 c11 c12
o6 c41
c41 h57 c41 h58 c41 h59
c12 o4 c12 h13 c12 c13
c13 h14 c13 o7 c13 c14
o7 c42
c42 h60 c42 h61 c42 h62
c14 h15 c14 h16 c14 c15
c15 h17 c15 c34 c15 c16
c34 h40 c34 h41 c34 h42
c16 h18 c16 h19 c16 c17
c17 c35 c17 c18
c35 h43 c35 h44 c35 h45
c18 h20 c18 c19
c19 h21 c19 c36 c19 c20
c36 h46 c36 h47 c36 c37
c37 h48 c37 c38
c38 h49 c38 h50
c20 o8 c20 c21
c21 h22 c21 h23 c21 c22
c22 h24 c22 o9 c22 c23
o9 h67
c23 h25 c23 c39 c23 c24
c39 h51 c39 h52 c39 h53
c24 o c24 h26 c24 c25
c25 c40 c25 c26
c40 h54 c40 h55 c40 h56
c26 h27 c26 c27
c27 h28 c27 c28 c27 c32
c28 h30 c28 h29 c28 c29
c29 h31 c29 o10 c29 c30
o10 c43
c43 h63 c43 h64 c43 h65
c30 o11 c30 h32 c30 c31
o11 h68
c31 h33 c31 h34 c31 c32
c32 h35 c32 h36
end

imphd
c8 c6 c7 o3
c7 n c6 o2
c1 o c o1
```

```
h27 c27 c26 c25
c24 c40 c25 c26
c19 c21 c20 o8
h49 h50 c38 c37
c36 h48 c37 c38
h20 c19 c18 c17
c16 c35 c17 c18
end
termatom * *
RESIDUE_END
```

Preparation of the starting structures of the FKBP12 complexes

The equilibrium simulations for the complex involving the FKBP12 native state were started from the experimental structure[3] (PDB code 1FKJ) for the FK506-FKBP12 pair and from the experimental structure[4] (PDB code 1FKG) for the SB3-FKBP12 pair. The starting configuration for the N-Elte378-FKBP12 complex (for which no experimental structure is available) was obtained by placing the α-keto amide moiety of the ligand in the same position of the corresponding unit in SB3 (i.e. with the two O3-H(OH)Tyr82 and O2-HN(Ile56) H-bonds, see Figure S2) and then optimizing the structure of the R and R' end groups of N-Elte378 in the FKBP12 pocket using conjugate gradient minimization. For the complexes with the FKBP12(I56D) mutant, the initial structures were prepared starting from the corresponding initial structures of the native FKBP12 complexes, optimizing the Asp56 side chain using conjugate gradient minimization. The FKBP12 complexes were accommodated in a tetragonal box ($a = 4.5$ nm, $b = 6.0$ nm) with the axis bearing the smallest the inertia moment of the FKBP12 molecule approximately aligned along the major axis of the box. The box was then uniformly filled with randomly oriented TIP3P water at the density of 1 g/cm^3. Water molecules overlapping with protein or ligand atoms were discarded. Prior to launch the EDU-HREM simulation, the solvated complexes were equilibrated using standard MD for 100 ps in the NPT ensemble (T=300 K and P=1 atm), with a strong tethering harmonic potential (force constant 100 kcal mol^{-1} Å^{-2}, equilibrium distance 1.9 Å) between the hydroxy hydrogen of Tyr82 and the O3 of the ligand to prevent adventitious detachment of the ligand while

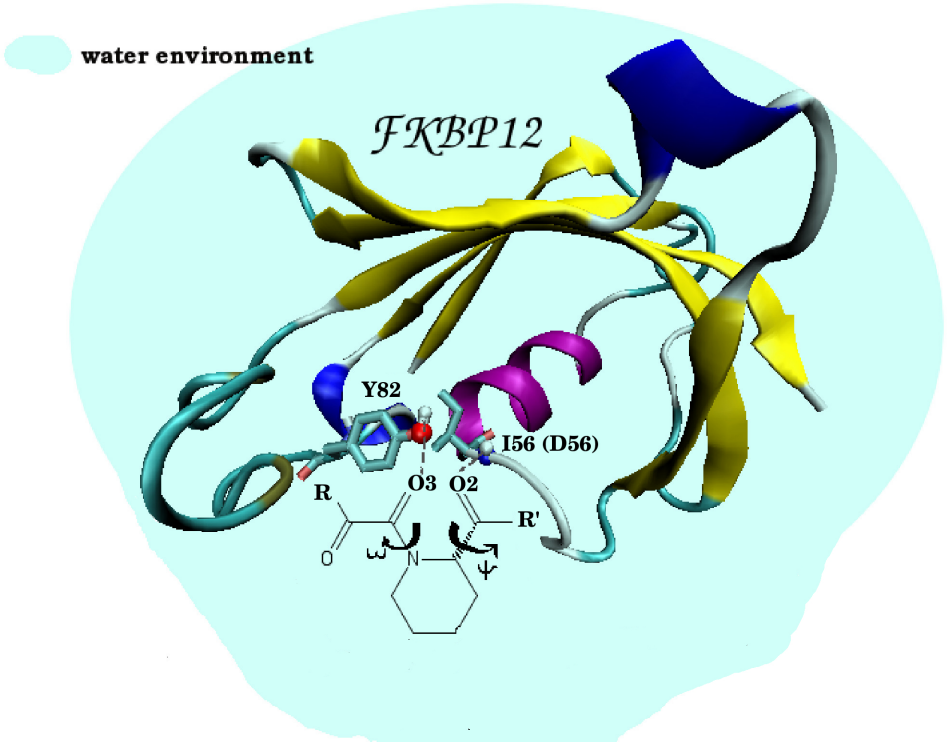

Figure S2: FKBP12 binding pocket with the α-keto amide moiety of a FK506-related ligand. The H-bonds involving the ligand and I/D56 and Y82 residues are also shown. The ω and ψ dihedral angles in the FKBP12 co-crystals with FK506-related ligands[3,4] correspond to, approximately, *trans* and *cis* rotameric states.

equilibrating the solvent.

EDU-HREM scaling protocol for the FKBP12 bound states

Here we present the basic aspects of the EDU-HREM simulation setup. A detailed description of the EDU-HREM method is reported in Ref.[5] The solute comprises: whole ligand, Tyr26, Phe36, Phe46, Val55, Ile/Asp56, Trp59, Tyr82, Ile90, Ile91, Leu97, Phe99, Hse87, Pro88, Gly89, Glu54. The total number of atoms scaled in each system is: 377 (370) for SB3-native (mutated) protein; 325 (318) for N-Elte378-native (mutated) protein; 397 (390) for FK506-native (mutated) protein (see the example of FK506-FKBP12 in Figure S3). The total number of atoms in the system, including water, is about 12000. Only intrasolute interactions are scaled replica progression. The solute-solute term is further split into three contributions with different scaling factors: 1) $v_{stretch} + v_{bend} + v_{i-tors}$; 2) $v_{p-tors} + v_{1-4}$ and 3) v_{nb}. We did not scale the potential related to stiff degrees of freedom (stretchings, bendings and improper torsions). We only scaled the proper torsions and fudged 1-4 potential terms ($v_{p-tors} + v_{1-4}$) from 1 (target replica) down to 0.25 (corresponding to a temperature of 1200 K) and the intrasolute non bonded potential v_{nb} from 1 (target replica) down to 0.3 (corresponding to a temperature of 1000 K). This scaling protocol was implemented along a progression of 16 replicas as shown in Figure S3 (right panel). The EDU-HREM simulations for the complexes were done for 5 ns in all cases at T=300 K and P=1 atm, with the tethering potential force constant set to 0.02 kcal mol $^{-1}$ Å^{-2}. Average a and $b = c$ axis of the tetragonal box were at 58.4 Å and 43.9 Å.

The contact function $H(\mathbf{x})$, expressing the number of protein residues in contact with the ligand at a given configurational state $\mathbf{x}$ in the GE ensemble, is given by

$$H(\mathbf{x}) = \sum_{j=1}^{N_{\text{residues}}} \Theta(r_d - r_j(\mathbf{x})) \tag{11}$$

where N_{residues} is the number of residues in the protein, $r_j(\mathbf{x})$ is the "distance" between the residue j and the ligand. The "distance" between the j-th residue and the ligand is defined as $r_j = \min(|\mathbf{r}_{jk} -$

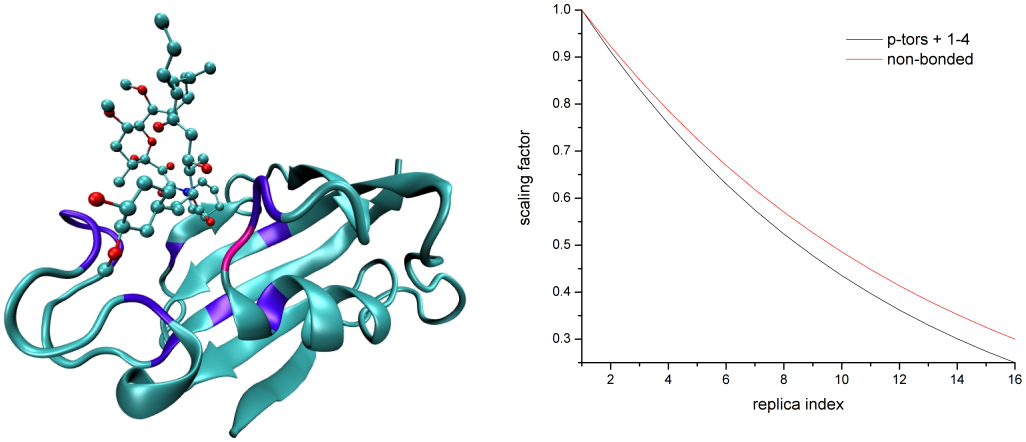

Figure S3: *Left*: Initial configuration of FKBP12-FK506 complex (no hydrogen atoms). Scaled residues are in violet. Ile56, also scaled, is shown in magenta. *Right*: Scaling factor values along replica progression.

$\mathbf{r}_l|)$ where the index l and k run on the atoms of the ligand and of the j-th residue, respectively. $\Theta(r_d - r_j(\mathbf{x}))$ is the Heaviside step function. The threshold distance r_d for a contact depends on the residue type, polar (4 Å) , non polar (5 Å) and planar/aromatic (5.5 Å). In Figure S4, we show the probability distribution of the contact function $H(\mathbf{x})$ for various GE states including the target state and the state corresponding to the "hottest" replica.

Binding pattern for the FKBP12(native and I56D) bound states

In the Figure S5 the atom-atom distance distribution functions for the most persistent contacts in the ligand-FKBP12 bound states are shown. For all ligands, the H-bond contacts involving the Tyr87 and Ile/Asp56 residue and the contact involving Trp59 and the C3 atom (1FKG atom indexing) of the pipecolic moiety are very stable in native FKBP12 (left plots) with sharp distribution function peaked around 2 and 4 Å, respectively. When Ile56 is mutated to Asp56 (right panel), the sharp pattern based on these three contacts is erased with new hydrophobic contacts (Ile97 in SB3 and Phe36 in N-Elte378) stabilizing the bound state. Remarkably, in the FK506-FKBP12(I56D) complex, the binding pattern seen in native FKBP12, while being significantly perturbed, is essentially preserved.

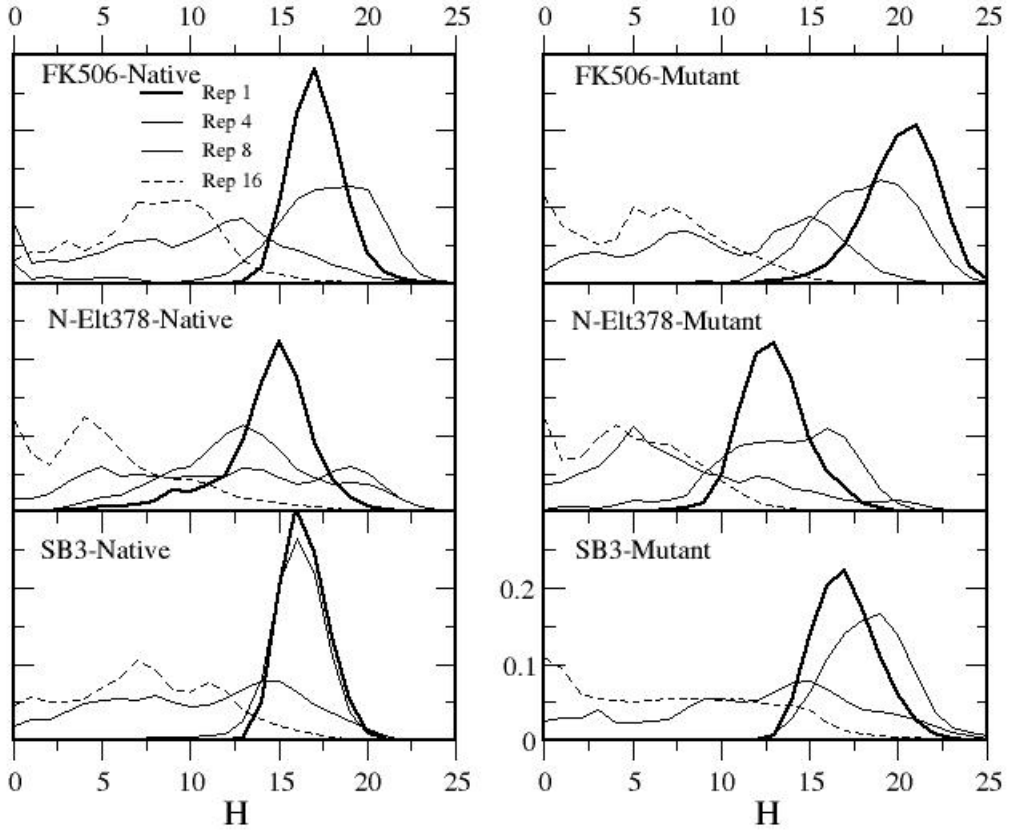

Figure S4: Probability distribution functions of the contact function (Eq.(11)) for the various FKBP12 native (left plots) and I56D mutant (right plots) complexes as obtained in a 5 ns of 16 replicas generalized ensemble simulation. At the target state (replica 1) the contact function is peaked at the average number of residues in contact with the ligand (see Eq. 11), showing that the ligand is in all cases tightly bound in the FKBP12 pocket. For "high-temperature" replicas the contact function is broader showing an enhanced probability for a detachment of the ligand from the binding site.

The FK506-FKBP12(I56D) system

The FK506-FKBP12(I56D) complex exhibits an extremely high binding free energy (calculated assuming a normal distribution of the work for the annihilation of FK506 in the bound state and in the bulk) yielding a dissociation constant in the femtomolar range. To further check this unexpected result, we have extended the EDU-HREM simulation for the FK506-FKBP12(I56D) complex for additional 2.5 ns harvesting a new set of 256 equilibrium initial configurations. In Figure S6 we report the time record of the moments of the distributions using three sets of 256 NE trajectories

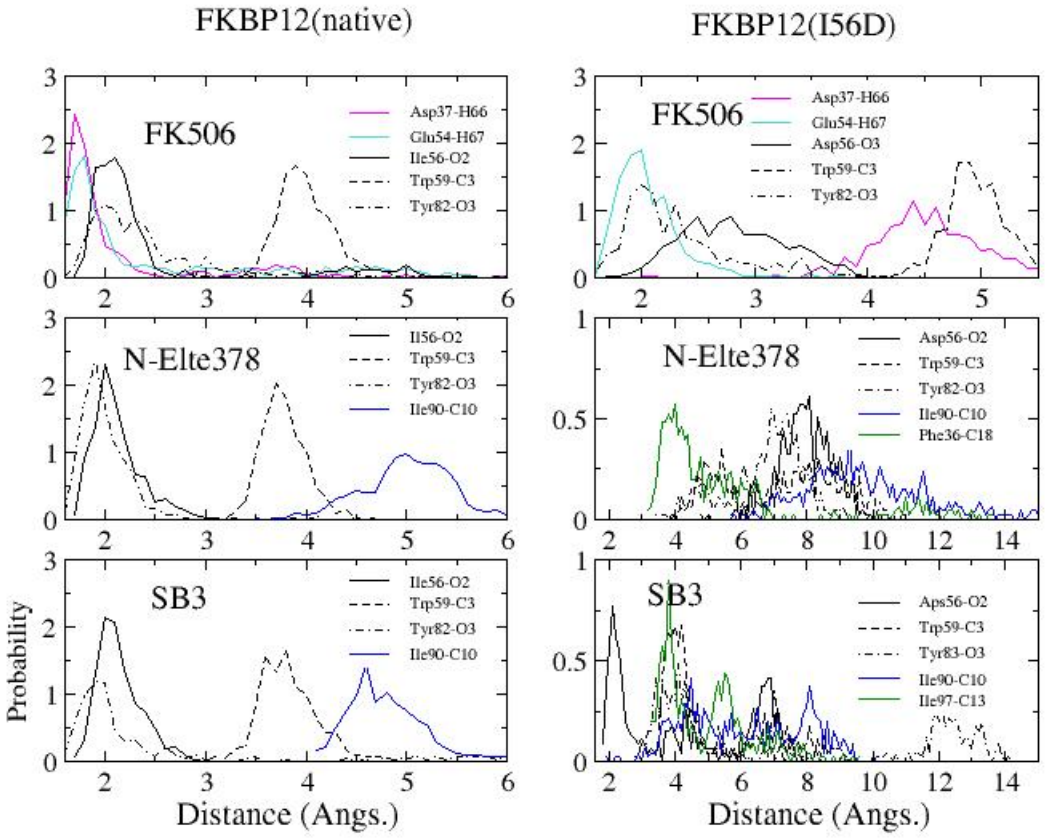

Figure S5: Distribution functions of the distance between selected protein and ligand atoms (1FKG and 1FKJ atom indexing) for the bound state of all examined complexes using 512 configurations uniformly sampled in the target replica.

that were started from three consecutive equally lasting pieces of the EDU-HREM simulations. Apparently the work distributions look very similar (see Figure S6, left panel). Indeed, as shown in Figure S6 (right), the first moment $\langle W_{1\to 0}(\tau)\rangle$ is virtually identical at all times of the annihilation process. The main differences are observable in the width of the distributions that in the case of the last sample is significantly larger leading to a moderate decrease in the annihilation free energy as computed assuming a single normal distribution of the work, $\Delta G_b = \langle W^{(b)}_{1\to 0}(\tau)\rangle - \beta\sigma_b^2/2$. The final annihilation works of FK506-FKBP12(I56D) complex passed the Kolmogorov-Smirnov test with a reference underlying normal distribution $N(W) = (\frac{1}{2\pi\sigma^2})^{1/2} e^{-(W-\langle W_{1\to 0}\rangle)^2/(2\sigma^2)}$, like for all other systems with the exception of N-Elte378 in bulk (see discussion of Figure 3 of the paper).

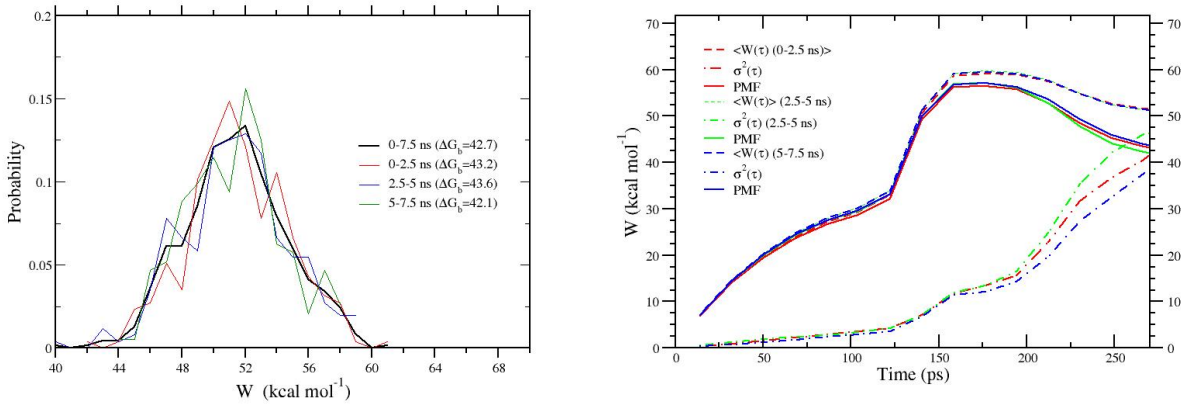

Figure S6: Left panel: work distributions ($\tau = 270$) obtained using NE trajectories started from consecutive pieces of the equilibrium EDU-HREM simulation for the FK506-FKBP12(I56D) system. Right panel: moments of the work distribution as a function of the annihilation time.

Nonetheless, based on the observation of the σ trends reported in Figure S6(right), we may suspect the existence of a secondary component in the final annihilation work distribution for FK506-FKBP12(I56D) with larger σ due to a manifold of alternative poses in the FKBP12(I56D) binding site. We therefore computed again the free energy using a mixture of *two* normal distributions for *all* systems by means of the Crooks-based relation:

$$\Delta G_{2\mathrm{G}} = -k_B T \ln \left[c_1 e^{-\beta(W_1 - \beta\sigma_1^2/2)} + c_2 e^{-\beta(W_2 - \beta\sigma_2^2/2)} \right] \tag{12}$$

in alternative of the standard single-component estimator

$$\Delta G_{1\mathrm{G}} = W_1 - \beta\sigma^2/2 \tag{13}$$

While there are no fitting parameters in Eq. 13, the weights c_1 and $c_2 \equiv 1 - c_1$ in Eq. 12 and the moments W_1, W_2, σ_1, σ_2 are fitted according to the procedure described in Ref.[6] Results obtained for the 2G-free energies for all ligands in bulk and in the complexes are reported in Table S1. In parenthesis the 1G-counterpart is also reported, taken from Table 2 of the main paper. From inspection of Table S1, we first notice that the bootstrap errors in the 2G-fit are definitely much

Table S1: Dissociation free energies in FKBP12 (native and I56D mutant) complexes for some FK506-related ligands computed using a 2G and 1G (in parenthesis) estimates of the annihilation free energies (Eqs 12 and 13, respectively). Note that for N-Elte378 in bulk we computed the annihilation free energy using only the 2G fit (see main paper). $\Delta G_{b0} = \Delta G_b + k_B T \ln(V_{\rm site}/V_0)$ is the annihilation free energy of the ligand in the bound state including a SSC correction of -0.2 ± 0.1 kcal mol^{-1}. ΔG_s is the annihilation free energy of the free ligand in bulk. All units are in kcal mol^{-1}. Errors are evaluated by block-bootstrapping 40 random sample containing 256 works from the complete set of 512 work values

	ΔG_{b0}	ΔG_s	$\Delta G_0^{\rm FS-DAM}$
FK506(native)	32.4(33.0)$\pm$1.1(0.7)	20.2(20.4) $\pm$0.3(0.1)	12.2(12.6) $\pm$1.4(0.8)
FK506(I56D)	**36.7**(42.5)$\pm$3.4(0.4)	20.2(20.4) $\pm$0.3(0.1)	**16.5**(22.1) $\pm$**3.7**(0.5)
N-Elte378(native)	22.5(22.5)$\pm$0.3(0.1)	9.8 $\pm$0.4	12.7(12.7) $\pm$0.7(0.5)
N-Elte378(I56D)	17.6(17.9)$\pm$1.1(0.1)	9.8 $\pm$0.4	7.8(8.1) $\pm$1.5(0.5)
SB3(native)	18.6(18.5)$\pm$0.6(0.3)	6.1(6.3) $\pm$0.3(0.1)	12.5(12.2) $\pm$0.9(0.4)
SB3(I56D)	17.1(17.3)$\pm$0.6(0.3)	6.1(6.3) $\pm$0.3(0.1)	11.0(11.0) $\pm$0.9(0.4)

higher than those corresponding to the 1G-fit (reported in parenthesis). This is in some sense expected as the fit of the $c_1 = 1 - c_2$ coefficient and of the moments of the mixture becomes ill-conditioned when there is no real evidence for a bimodal distribution.[6] It should also be remarked that only in the case of the complex FK506-FKBP12(I56D) the 2G-fit yields an annihilation free energy that is significantly different from that obtained in the 1G-fit. In all other cases, the 2G-fit and 1G-fit produce in general quite similar results with maximum discrepancy of only 0.3 kcal mol^{-1}. The 2G-fit annihilation free energy for FK506-FKBP12(I56D) is 16.5$\pm$3.7 kcal mol^{-1}, 5.6 kcal mol^{-1} below the annihilation free energy of FK506 found in the native protein of 22.1$\pm$0.5. The error on the 2G-fit value for the FK506-FKBP12(I56D) system is by far the highest of all annihilation 2G-free energies (nearly 4 kcal mol^{-1}) indicating severe ill-conditioning with free energies found in the random independent bootstrap samples ranging from 33 to 43 kcal mol^{-1}. Assessing more precisely the incidence of secondary components due to alternative poses in the the dissociation free energy of the FK506-FKBP12(I56D) complex is a matter that requires further study and extensive computations. Here, it suffices to say that, to reduce the error by a factor of four (thus providing a confidence for the dissociation free energy within 1 kcal mol $^{-1}$), one needs to produce, to the least, ten times more NE trajectories. Correspondingly, the EDU-HREM

equilibrium simulation should be extended ten times longer than the 5 ns used in the present study.

References

(1) Procacci, P. Unpublished.

(2) Marsili, S.; Signorini, G. F.; Chelli, R.; Marchi, M.; Procacci, P. *J. Comp. Chem.* **2010**, *31*, 1106–1116.

(3) Wilson, K. P.; Yamashita, M. M.; Sintchak, M. D.; Rotstein, S. H.; Murcko, M. A.; Boger, J.; Thomson, J. A.; Fitzgibbon, M. J.; Black, J. R.; Navia, M. A. *Acta Crystallographica Section D* **1995**, *51*, 511–521.

(4) Holt, D. A.; Luengo, J. J. I.; Yamashita, D. S.; Oh, H. J.; Konialian, A. L.; Yen, H. K.; Rozamus, L. W.; Brandt, M.; Bossard, M. J.; Levy, M. A.; Eggleston, D. S.; Liang, J.; Schultz, L. W.; Stout, T. J.; Clardyt, J. *J. Am. Chem. Soc.* **1993**, *115*, 9925–9938.

(5) Procacci, P.; Bizzarri, M.; Marsili, S. *J Chem. Theory Comp.* **2014**, *10*, 439–450.

(6) Procacci, P. *The Journal of Chemical Physics* **2015**, *142*, 154117.